Journal of Molecular Graphics and Modelling 51 (2014) 113–119

Contents lists available at ScienceDirect

Journal of Molecular Graphics and Modelling

journal homepage: www.elsevier.com/locate/JMGM

A QM/MM study of the catalytic mechanism of aspartate ammonia lyase

Jing Zhang[a,b], Yongjun Liu[b,c,*]

[a] Key Laboratory of Inorganic Chemistry in Universities of Shandong (Jining University), Qufu, Shandong 273155, China
[b] Northwest Institute of Plateau Biology, Chinese Academy of Sciences, Xining, Qinghai 810001, China
[c] School of Chemistry and Chemical Engineering, Shandong University, Jinan, Shandong 250100, China

ARTICLE INFO

Article history:
Accepted 5 May 2014
Available online 14 May 2014

Keywords:
Aspartate ammonia lyase
QM/MM
Mutation
Reaction mechanism
L-aspartate.

ABSTRACT

Aspartate ammonia lyase (Asp) is one of three types of ammonia lyases specific for aspartate or its derivatives as substrates, which catalyzes the reversible reaction of L-aspartate to yield fumarate and ammonia. In this paper, the catalytic mechanism of Asp has been studied by using combined quantum-mechanical/molecular-mechanical (QM/MM) approach. The calculation results indicate that the overall reaction only contains two elementary steps. The first step is the abstraction of C_β proton of L-aspartate by Ser318, which is calculated to be rate limiting. The second step is the cleavage of C_α—N bond of L-aspartate to form fumarate and ammonia. Ser318 functions as the catalytic base, whereas His188 is a dispensable residue, but its protonation state can influence the active site structure and the existing form of leaving amino group, thereby influences the activity of the enzyme, which can well explain the pH dependence of enzymatic activity. Mutation of His188 to Ala only changes the active site structure and slightly elongates the distance of C_β proton of substrate with Ser318, causing the enzyme to remain significant but reduced activity.

1. Introduction

Ammonia lyases catalyze the cleavage of C—N bonds without employing hydrolysis or oxidation mechanisms. Aspartate ammonia lyase, also known as aspartase (Asp, EC 4.3.1.1), is one of the three types of ammonia lyases specific for aspartate or its derivatives as substrates [1,2]. It catalyzes the reversible conversion between L-aspartate and fumarate, as shown in Scheme 1 [3], and plays an important role in microbial nitrogen metabolism. In industry, Asp is used as biocatalyst for the production of L-aspartate, which is an important precursor for the synthesis of food additives and artificial sweeteners [4]. Asp belongs to the aspartase/fumarase superfamily, which is a group of homologous proteins sharing common tertiary and quaternary fold and similar active site architecture, although the pairwise sequence identities can be as low as 15% [5]. Asps have been purified and characterized from a number of Gram-positive and Gram-negative bacteria. Among them, the best studied Asps are from *Escherichia coli* (AspA) and *Bacillus* sp. YM55-1 (AspB) [3,4,6–12]. Compared with AspA, AspB has raised great biocatalytic interest in organic synthesis owing to its high activity and enantioselectivity, broad nucleophile specificity, relative thermostability and lack of allosteric regulation by substrates or metal ions [9,10,12].

Many experimental studies have been conducted to investigate AspB, and some crystal structures have been obtained [3,4,9–11]. In 2011, G. Fibriansah and coworkers reported the crystal structures of AspB both in unliganded state and in complex with L-aspartate at 2.4 and 2.6 Å resolutions (PDB code: 3R6Q and 3R6V), respectively [4]. Similar to other members of aspartase/fumarase superfamily, the functional unit of AspB is also a homotetramer, as shown in Fig. 1. The monomeric subunit is composed of three main α-helical domains: the N-terminal domain (residues 5–139), the central helix domain (residues 140–393), and the C-terminal domain (residues 394–466). Residues from three different subunits form one active site, and totally four active sites can be found in a tetrameric molecule. The SS loop (residues 317–328) from one of the three subunits closes over the active site when substrate L-aspartate presents in the active site, therefore, it involves in substrate binding, as shown in Fig. 2a. It is interesting to note that the substrate L-aspartate adopts its energetically unfavorable rotamer in which the C_α, C_β, and β-carboxylic atoms are almost coplanar, as shown in Fig. 2. The reason is that residues in active site form an exten-

Abbreviations: Asp, aspartate ammonia lyase; AspA, aspartate ammonia lyase from *Escherichia coli*; AspB, aspartate ammonia lyase from *Bacillus* sp. YM55-1; His188Ala mutant, the alanine mutant of His188; PDB, Protein Data Bank.

* Corresponding author at: Northwest Institute of Plateau Biology, Chinese Academy of Sciences, Xining, Qinghai 810001, China. Tel.: +86 531 88365576; fax: +86 531 88564464.
E-mail address: yongjunliu_1@sdu.edu.cn (Y. Liu).

http://dx.doi.org/10.1016/j.jmgm.2014.05.003
1093-3263/

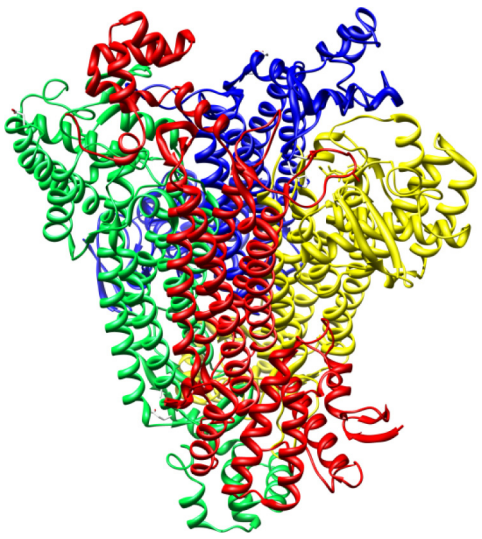

Fig. 1. Overall structure of AspB. Four subunits are colored yellow, blue, red, and green, respectively. (For interpretation of the references to color in this figure legend, the reader is referred to the web version of the article.)

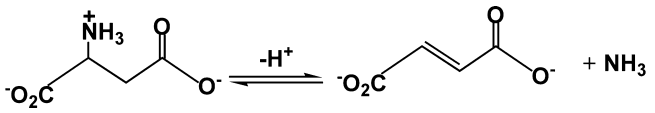

Scheme 1. The reversible reaction of L-aspartate to yield fumarate and ammonia catalyzed by aspartate ammonia lyase.

sive hydrogen bond network with L-aspartate which can make L-aspartate keep this high-energy state.

These three-dimensional structures provide new insights into the catalytic mechanism of aspartate ammonia lyase. Previous studies indicate that members of aspartase/fumarase superfamily use the common catalytic strategy as shown in Scheme 2: the general base of the enzyme firstly abstracts a proton from the C_β atom of L-aspartate, producing an enediolate intermediate; then, the C_α—N bond of the substrate cleaves to form fumarate and ammonia, and the cleavage of C_α—N bond can be facilitated by a general acid to protonate the leaving ammonia [13–19]. It is suggested that the substrate L-aspartate adopts a high-energy conformation, in which a hydrogen bond network is formed between the closed SS loop and pocket residues, facilitating the formation of enediolate-like transition state and enediolate intermediate [4]. The important role of SS loop in catalysis has been proved by the crystal structure as well as mutant experiments [3,4]. The closure conformation of SS loop is favorable for the approach of Ser318 to the C_β proton of L-aspartate to abstract it [4]. Mutation of Ser318 to an alanine demonstrated a complete inactivation of the enzyme. Therefore, Ser318 is assumed to be functional as a catalytic base. Lys324 is also suggested to be an essential residue, because mutations at this position always cause a complete loss of activity. Besides Ser318 and Lys324, another highly conserved residue in this superfamily is His188. The alanine mutant of His188 (His188Ala) retains a significant activity and displays an unchanged pH rate profile compared to wild type AspB. The catalytic importance of other residues such as Thr101, Ser140, Thr141, Asn142 and Thr187 has also been judged by site-directed mutagenesis [3].

Although a rough picture of the catalytic mechanism has been obtained, open questions still remain. The detailed reaction pathway, the roles of pocket residues, and the energetics of whole catalytic cycle are still not fully understood. Moreover, His188 is in proximity to the leaving group (ammonia), which may function as general acid to protonate the ammonia to help its release. But experiments indicated that His188Ala still displays a significant activity [3], implying His188 is not necessary for C_α—N bond cleavage. Therefore, the role of His188 in chemical process and its role in the releasing step of ammonia are still unclear [5].

In the present work, we employed the combined quantum mechanics and molecular mechanics (QM/MM) method to study the proposed catalytic mechanism of aspartate ammonia lyase [20–23]. The key point of the QM/MM approach is to divide the entire system into two portions, QM region and MM region. The QM region involving the formation and cleavage of chemical bonds is described quantum mechanically, while the MM region representing the surrounding protein is described by the classical molecular mechanics. This methodology can take both the chemical reaction occurred in active site and the effect of protein and solvent environment into consideration, and has been extensively applied in the studies of enzymatic reaction mechanism [24–28]. Based on the crystal structure determined by G. Fibriansah, the reaction models were constructed, and the reaction barriers and energies were calculated. Moreover, the role of key pocket residues was illuminated.

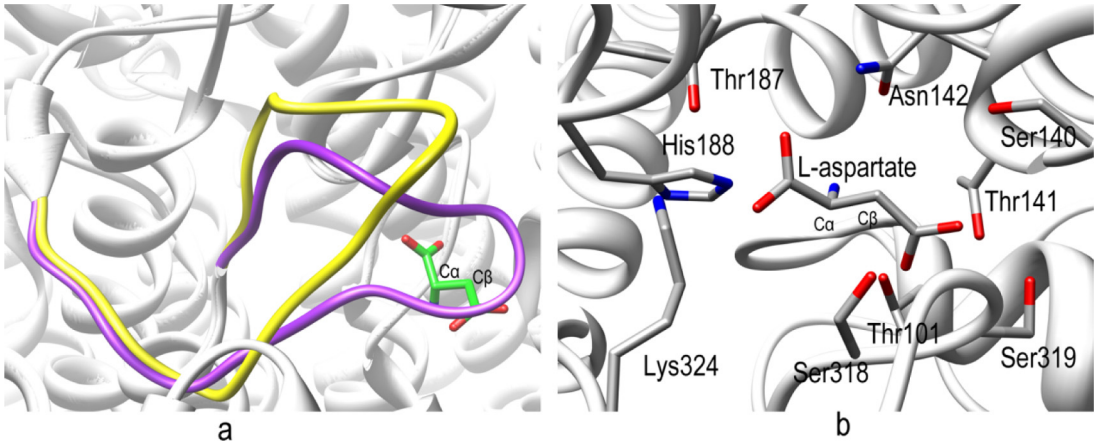

Fig. 2. (a) Superposition of the SS loop of AspB in the unliganded state and in complex with L-aspartate (yellow, unliganded, open conformation; purple, complex with L-aspartate, closed conformation). (b) The active site of AspB in complex with L-aspartate in crystal structure.

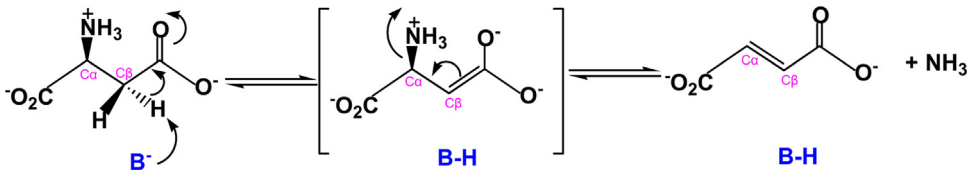

Scheme 2. Proposed catalytic mechanism of aspartate ammonia lyase for the reversible L-aspartate dissociation.

2. Computational details

2.1. Computational model

The structure of AspB in complex with L-aspartate was constructed following the crystallographic atomic coordinate taken from Protein Data Bank (PDB ID code: 3R6V) [4]. The protonation states of all ionizable residues were determined according to the experimental condition and their p*K*a values were predicted by PROPKA 3.1 program [29]. But for the important residue His188, both the deprotonated and protonated states were considered. Ser318 is assumed to function as a catalytic base, so it was deprotonated in our models. The protonation states of all residues were checked carefully by the VMD program [30]. The missing hydrogen atoms were added by means of the HBUILD facility in the CHARMM package [31]. Each system was solvated into a water sphere with a 46 Å radius in which the water molecules were treated as TIP3P residues [32]. Then each system was neutralized by adding Na^+ ion at random position. The prepared system was equilibrated with a series of minimizations and a 2 ns MD simulation by using the CHARMM22 force field [33].

2.2. QM/MM calculations

The QM/MM calculations were performed with the ChemShell software package [34], which integrates the TURBOMOLE package [35] for QM subsystem and DL-POLY program [36] for MM subsystem. The resulting QM/MM system has a total of ~31,000 atoms. The QM subsystem contains the substrate L-aspartate and some important residues in the active site, including His188 and Thr187 from chain A, Thr101, Ser140, Thr141 and Asn142 from chain B, and Ser318, Lys324, and Ser319 from chain C. These QM atoms were treated with B3LYP functional and 6-31G(d,p) basis set [24,25,37,38]. All the other atoms were assigned to MM subsystem, which were described at CHARMM22 force field [39]. During the calculations, the QM atoms and parts of the MM atoms within a distance of 10 Å from L-aspartate were allowed to move freely and were fully optimized, whereas the remaining MM atoms were fixed. The electronic embedding scheme and the hydrogen link atoms with charge shift model [40] for QM/MM boundary were applied in the QM/MM treatment. There was no cutoff introduced for the nonbonding MM and QM/MM interactions. Geometry optimizations were implemented by Hybrid delocalized internal coordinates (HDLC) optimizer [41], and a quasi-Newton limited

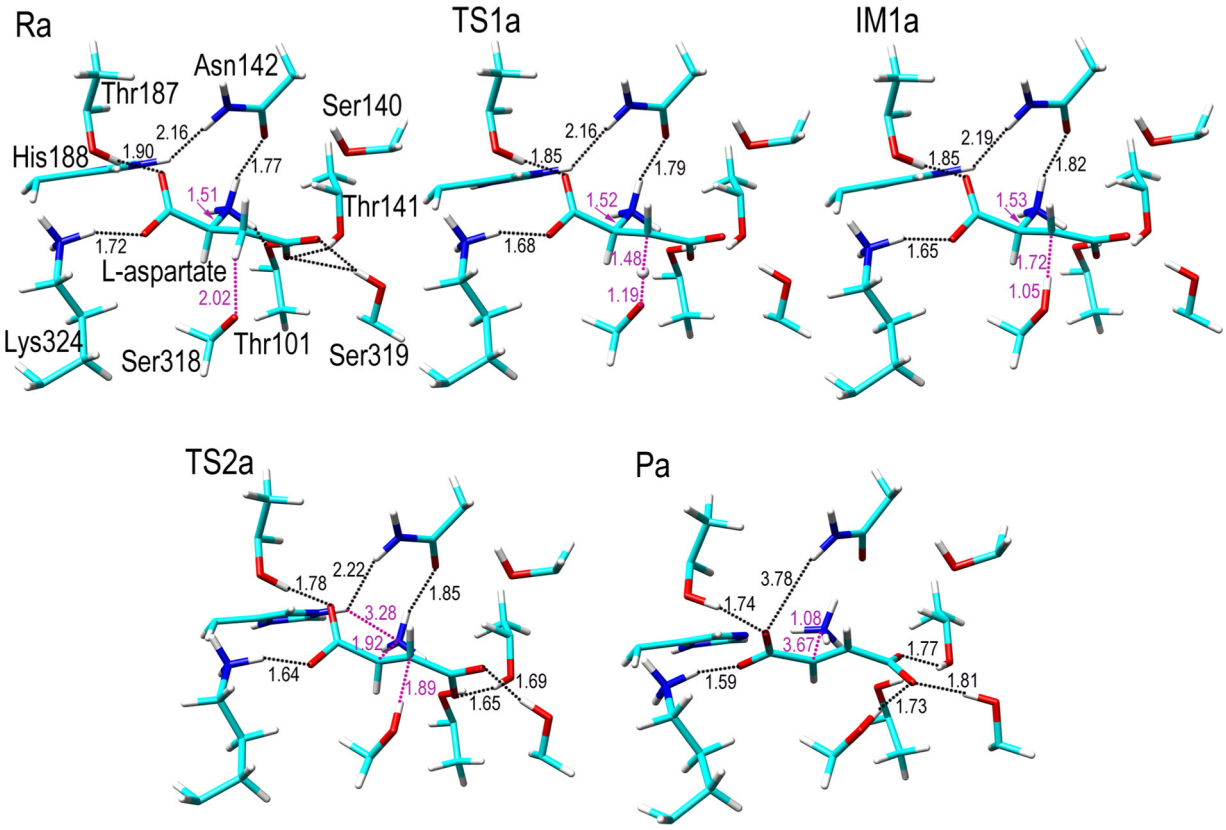

Fig. 3. QM/MM optimized active structures of reactant (Ra), transition states (TS1a, TS2a), intermediate (IM1a), and product (Pa) when His188 is in protonated state. Distances are given in Å.

memory Broyden–Fletcher–Goldfarb–Shanno (L-BFGS) algorithm [41] was used to search for minima. The prepared QM/MM system was employed to search for the optimal energy path with the QM/MM-scanned energy mapping method. The transition states were taken from the highest points on the potential energy profile along the reaction coordinate and then optimized with partitioned rational function optimization (P-RFO) method [41], which then checked by further optimization calculations to confirm their connections between the corresponding intermediates. Finally, single-point QM/MM calculations were performed with larger basis set 6–31++G(d,p) on the 6–31G(d,p) optimized geometries to obtain accurate energies.

3. Results and discussion

3.1. Structure of enzyme-substrate complex

The initial crystal structure of AspB in complex with L-aspartate is shown in Fig. 1, and the active pocket with the key surrounding residues is shown in Fig. 2b. After a serial of MD simulations and QM/MM optimization, the final QM/MM optimized structure, denoted as reactant (Ra) is shown in Fig. 3. By comparative analysis, we see that the relative positions of active residues are similar to those of crystal structure, and the calculated root-mean-squared deviations (RMSD) of the QM/MM optimized structure relative to crystal structure are only 0.63 Å. The α-amino group of L-aspartate forms two hydrogen bonds with the side chains of Thr101 and Asn142. The α-carboxylate group makes three hydrogen bonds with the side chains of Asn142, Thr187, and Lys324. Further, the protonated amino of Lys324 forms a salt-bridge with the α-carboxylate group of L-aspartate, thereby stabilizing the substrate. Moreover, the β-carboxylate group of L-aspartate forms intricate hydrogen bonds with Thr101, Thr141, Ser319 and α-amino group of L-aspartate. In addition to its role in substrate binding, this extensive hydrogen bonding network appears to be important for stabilizing the additional negative charge on the coming enediolate transition state or intermediate. The hydrogen bond length between Ser318 and the C_β proton of L-aspartate is 2.02 Å, which is favorable for the subsequent proton transfer. All the above bonds construct a large hydrogen bonding network and the substrate is tightly bound to the active site in its energetically unfavorable rotamer. This structure is used as the initial reactive state for the QM/MM calculations of the reaction mechanism.

3.2. Reaction path

According to the previously proposed catalytic mechanism, we studied the reaction details of AspB. On the basis of our calculations, the overall reaction cycle includes two elementary steps. The first one is the proton abstraction of C_β atom of L-aspartate by Ser318, generating the enediolate intermediate. The next step is the cleavage of C_α–N bond of L-aspartate to form fumarate and ammonium cation.

The optimized structures of transition states (TS1a and TS2a), intermediate (IM1a) and product (Pa) are shown in Fig. 3. In TS1a, the distance between the C_β proton of L-aspartate and hydroxyl oxygen ion of Ser318 decreases to 1.19 Å from 2.02 Å in Ra. In IM1a, this distance further shortens to 1.05 Å to form an O—H bond. In this elementary step, the relative positions of the substrate and its surrounding residues are almost unchanged, and the hydrogen binding network in the active site is well kept. The next step is the cleavage of the C_α—N bond of L-aspartate. In TS2a, the single C_α—N bond weakens from 1.53 Å to 1.92 Å and His188 is still in its protonated state. But in Pa, the protonated His188 has denoted its proton to the released ammonia with the leaving group is ammoniumion (NH_4^+) rather than ammonia molecule (NH_3). Besides, residue Ser318 changes its orientation to the β-carboxylate group to form a hydrogen bond with length of 1.73 Å. We also note that both the two carboxylate groups of the substrate rotate about 90°, leading the β-carboxylate group to be perpendicular to the α-carboxylate group. In this state, the hydrogen bond between the α-carboxylate and Asn142 no longer exists. By comparing the structures of IM1a, TS2a and Pa, we can see that the cleavage of C_α—N bond and the proton transfer from His188 to ammonia molecule take place in a concerted but not synchronous manner. The beginning of proton transfer is much later than the cleavage of C_α—N bond.

The energy profile of the overall reaction is shown in Fig. 4a. The values in brackets are the results that QM atoms were treated at the B3LYP/6–31G(d,p) level. To obtain accurate energies, we performed single-point QM/MM calculations with larger basis set 6–31++G(d,p) on the 6–31G(d,p) optimized geometries, and the results are shown without brackets. By comparison, we can see that the energies depend largely on the basis sets. Similar situation can be found in Fig. 4b and c. The energy barrier for the formation of IM1a is 11.49 kcal/mol, which is much larger than that of the cleavage of C_α—N bond (5.72 kcal/mol), implying the proton abstraction by Ser318 to be the rate limiting step of the overall reaction. The

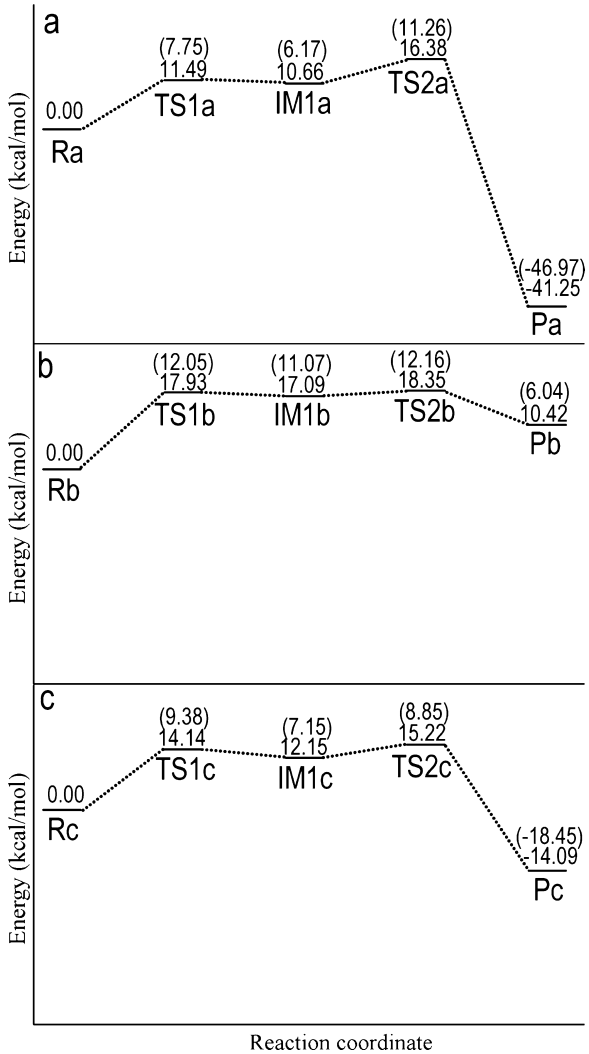

Fig. 4. Energy profile of the AspB catalytic process. (a) His188 is in protonated state; (b) His188 is in deprotonated state; (c) His188 is mutated to Ala. The values in brackets are the results that QM atoms were calculated at the B3LYP/6-31G(d,p) level, and the values without bracket are single-point QM/MM calculation results performed with larger basis set 6–31++G(d,p) on the 6-31G(d,p) optimized geometries.

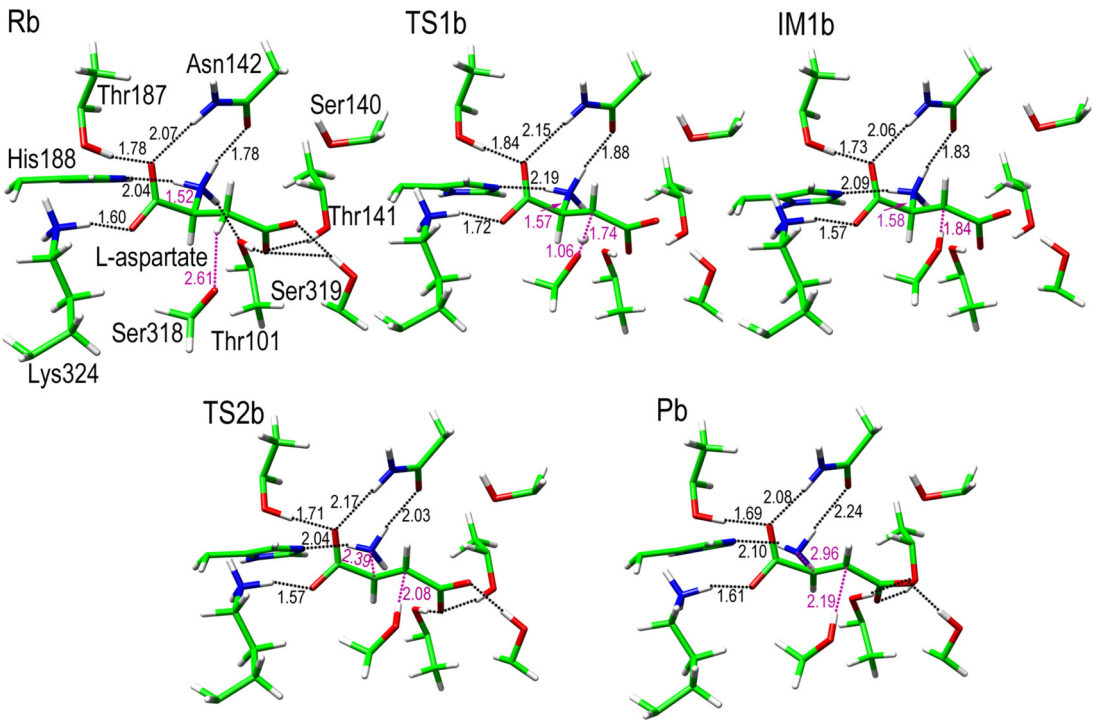

Fig. 5. QM/MM optimized active structures of reactant (Rb), transition states (TS1b, TS2b), intermediate (IM1b), and product (Pb) when His188 is in deprotonated state. Distances are given in Å.

estimated value of the free energy barrier from the experimental data is 15.27 kcal/mol [3], which is larger than our calculation result. In addition, the relative energy of Pa is 41.25 kcal/mol lower than that of Ra, meaning this reaction is highly exothermic. The reason why this step releases such an amount of heat is mainly due to the conformational change of the product fumarate. In Pa, the skeleton of fumarate no longer adopts its high-energy conformation. To verify this, we fixed the skeleton of fumarate in its high-energy conformation, the overall reaction is only exothermic by about 10 kcal/mol.

3.3. The influence of His188 in deprotonated state on reaction path

When His188 is in its deprotonated state, the QM/MM optimized structure of the reactant (Rb) is shown in Fig. 5. The binding mode of the substrate and key pocket residues is almost the same as Fig. 3 except some minor changes of bond lengths. Ser318 still forms hydrogen bond with the C_β proton of L-aspartate with length of 2.61 Å, which is longer than that in Ra (2.02 Å).

The optimized structures of transition states (TS1b and TS2b), intermediate (IM1b) and product (Pb) are shown in Fig. 5. In TS1b, the distance between the C_β proton of L-aspartate and hydroxyl oxygen atom of Ser318 changes to 1.06 Å from 2.61 Å. In IM1b, the C_β proton of L-aspartate has completely transferred to Ser318 with the formation of an enediolate intermediate. Then, in TS2b the C_α–N bond of L-aspartate elongates to 2.39 Å from 1.58 Å. In product Pb, the leaving group α-amino departs from the enediolate intermediate to form ammonia molecule. During the reaction process, the hydrogen binding mode remains unchanged except a slight twist of Thr101, which adjusts its orientation toward Thr141 to form a hydrogen bond with the hydroxyl oxygen of Thr141 in the final product (Pb).

The energy profile of the catalytic reaction is shown in Fig. 4b. One can see that the energy barrier for the formation of IM1b, the rate-limiting step, is much higher than that of IM1a (17.93 vs 11.49 kcal/mol). By comparing the structures of Ra and Rb, we found that the greatest difference between them is the distance of Ser318 with the C_β proton of L-aspartate. In Ra, this distance is only 2.02 Å, but in Rb it changes to 2.61 Å, which maybe the main reason to raise the energy barrier. In addition, Pb is 10.42 kcal/mol higher in energy than that of Rb, meaning this reaction is endothermic. Taking these results into account, we can conclude that His188 in protonated state is more favorable for the reaction. This conclusion coincides with the experimentally pH dependence of the kinetic parameters of AspB [3]. The authors proposed that a residue with a p*K*a of 9.8 must be protonated for optimal activity and functions as a general acid to protonate the leaving amino group [3].

3.4. Analysis of His188Ala mutant

Puthan Veetil et al. had mutated eight active site residues and demonstrated that most of the mutations led to the mutant enzymes with reduced or completely lost activities [3]. One exception is the mutant of His188Ala, which retained significant activity. To further understand the role of His188 in catalysis, we performed additional QM/MM calculations on the basis of His188Ala mutant. After mutation by VMD, MD simulation, and QM/MM optimization, we obtained the structure of His188Ala mutant in complex with substrate L-aspartate, which is denoted as reactant Rc, as shown in Fig. 6.

From the structure of Rc in Fig. 6 we can see that, compared with the wild type enzyme (Ra in Fig. 3), mutation of His188 to Ala188 only caused very slight structural changes in the active site. Notably, the distance between the C_β proton of L-aspartate and hydroxyl oxygen atom of Ser318 changes to 2.47 Å. In the proton abstraction process, this distance changes to 1.21 Å in TS1c. In IM1c, the C_β proton of L-aspartate is completely abstracted by Ser318 to form an enediolate intermediate. Then, the C_α-N bond of the substrate cleaved via TS2c to generate the final product (Pc). In Pc, the leaving α-amino group is in its neutral form (ammonia). Ser318 adjusts its

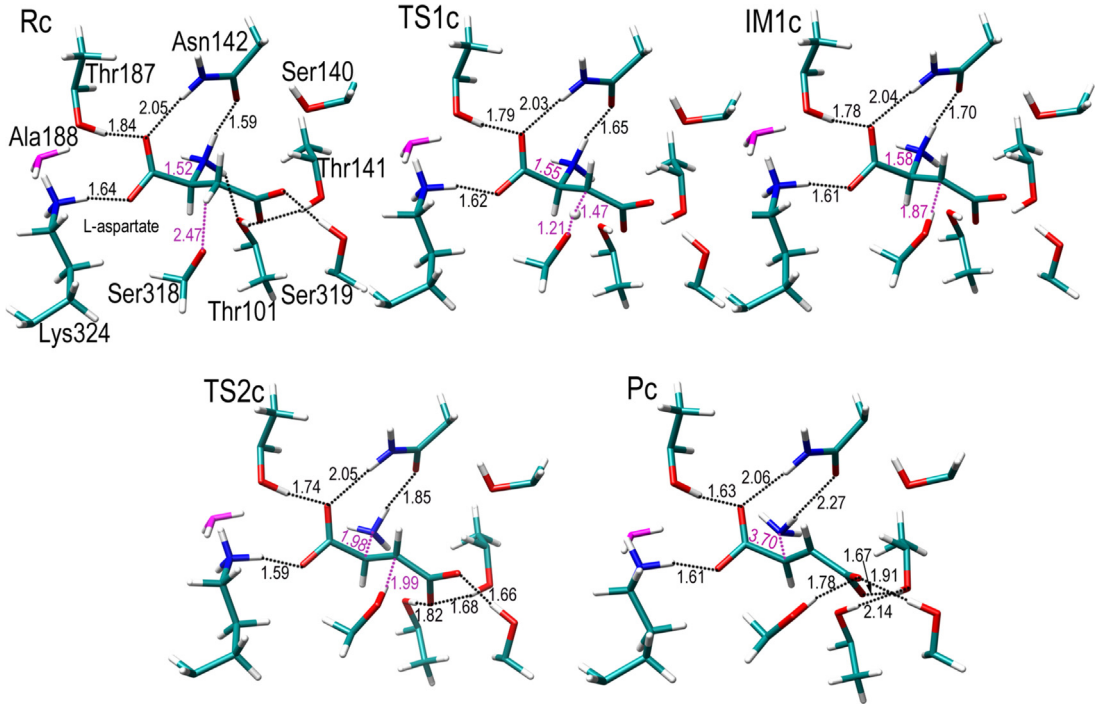

Fig. 6. QM/MM optimized active structures of reactant (Rc), transition states (TS1c, TS2c), intermediate (IM1c), and product (Pc) when His188 is mutated to Ala. Distances are given in Å.

orientation to form hydrogen bond with the β-carboxylate group of the substrate.

The energy profile is shown in Fig. 4c. Compared with the wild type enzyme, the energy barrier for the formation of IM1c is higher than that of IM1a but lower that of IM1b (14.14 vs 11.49 and 17.93 kcal/mol), which is in good agreement with experimental observation that His188Ala mutant showed reduced activity. In experiments, His188Ala mutant has an activity of approximately 57-fold reduction in the catalytic constant (kcat) and a 1.8-fold increase in the Michaelis constant (km), and an approximately 100-fold decrease in the rate constant (kcat/km) [3]. According to the experimental data, the estimated free energy barrier of His188Ala mutant is 17.66 kcal/mol, which is well consistent with our calculated result (14.14 kcal/mol). In addition, the relative energy of Pc is 14.09 kcal/mol lower than that of Rc, meaning this reaction is favorable in energy, and the product Pc is relatively stable.

By checking the structures of Ra, Rb and Rc, we found that the distances between the C_β proton of L-aspartate and hydroxyl oxygen atom of Ser318 are exactly proportional to the energy barriers of the first steps. In Ra, Rb and Rc, these distances are 2.02, 2.61, 2.47 Å, which correspond to the energy barriers of the first steps of 11.49, 17.93 and 14.14 kcal/mol, respectively. In Ra and Rb where His188 is in its protonated state or deprotonated state, due to minor changes of the active site structures, the distances between the C_β proton of L-aspartate and hydroxyl oxygen atom of Ser318 change, thereby influence the energy barriers of the proton abstraction process.

The calculation results suggest that His188 is not an absolute requirement for C_α—N bond cleavage, but the different protonation states of His188 impose different influence on active site structure and the leaving of amino group. Ser318 is very important to the catalytic reaction, which functions as a catalytic base to abstract the C_β proton of L-aspartate in the first step. It agrees well with the experiment that mutation of Ser318 to an alanine caused a complete inactivation of the enzyme [4]. When His188 is replaced by Ala, this enzyme keeps significant but reduced activity perhaps the active site structure was only slightly perturbed, and the leaving α-amino group is the neutral ammonia rather than the ammonium ion. This dispensable role of His188 was also found in other members of the superfamily [5].

4. Conclusions

The catalytic mechanism of aspartate ammonia lyase has been studied by using combined QM/MM approach. The calculation results indicate that the overall reaction only includes two elementary steps. The first step is the abstraction of the C_β proton of L-aspartate by Ser318, which is calculated to be rate limiting. His188, Thr187, Thr101, Ser140, Thr141, Asn142, Lys324, and Ser319 form extensive hydrogen bond network with the substrate, which plays important role in stabilizing the transition states and intermediates. Ser318 functions as the catalytic base to abstract the C_β proton atom of L-aspartate. His188 is a dispensable residue, but its protonation state can influence the active site structure and the existing form of leaving amino group, thereby influences the catalytic reaction. Because of the similar reason, the mutation of His188 to Ala only changes the active site structure and slightly elongates the distance of C_β proton of substrate with Ser318, therefore the enzyme remains significant but reduced activity. Besides, the different protonation states of His188 can influence the existing form of leaving amino group, which can well explain the pH dependence of enzymatic activity. These results may provide useful information for understanding the catalytic mechanism of AspB.

Acknowledgement

This work was supported by the Natural Science Foundation of China (21173129, 21373125).

References

[1] L. Poppe, J. Retey, Properties and synthetic applications of ammonia-lyases, Curr. Org. Chem. 7 (2003) 1297–1315.

[2] M. de Villiers, V. Puthan Veetil, H. Raj, J. de Villiers, G.J. Poelarends, Catalytic mechanisms and biocatalytic applications of aspartate and methylaspartate ammonia lyases, ACS. Chem. Biol. 7 (2012) 1618–1628.
[3] V. Puthan Veetil, H. Raj, W.J. Quax, D.B. Janssen, G.J. Poelarends, Site-directed mutagenesis, kinetic and inhibition studies of aspartate ammonia lyase from *Bacillus* sp. YM55-1, FEBS J. 276 (2009) 2994–3007.
[4] G. Fibriansah, V. Puthan Veetil, G.J. Poelarends, A.M. Thunnissen, Structural basis for the catalytic mechanism of aspartate ammonia lyase, Biochemistry 50 (2011) 6053–6062.
[5] V. Puthan Veetil, G. Fibriansah, H. Raj, A.M. Thunnissen, G.J. Poelarends, Aspartase/fumarase superfamily: a common catalytic strategy involving general base-catalyzed formation of a highly stabilized aci-carboxylate intermediate, Biochemistry 51 (2012) 4237–4243.
[6] R.E. Viola, L-Aspartase: new tricks from an old enzyme, Adv. Enzymol. Relat. Areas Mol. Biol. 74 (2000) 295–341.
[7] M.M. Jayasekera, W. Shi, G.K. Farber, R.E. Viola, Evaluation of functionally important amino acids in L-aspartate ammonia-lyase from *Escherichia coli*, Biochemistry 36 (1997) 9145–9150.
[8] W. Shi, J. Dunbar, M.M. Jayasekera, R.E. Viola, G.K. Farber, The structure of L-aspartate ammonia-lyase from *Escherichia coli*, Biochemistry 36 (1997) 9136–9144.
[9] Y. Kawata, K. Tamura, M. Kawamura, K. Ikei, T. Mizobata, J. Nagai, M. Fujita, S. Yano, M. Tokushige, N. Yumoto, Cloning and over-expression of thermostable *Bacillus* sp. YM55-1 aspartase and site-directed mutagenesis for probing a catalytic residue, Eur. J. Biochem. 267 (2000) 1847–1857.
[10] Y. Kawata, K. Tamura, S. Yano, T. Mizobata, J. Nagai, N. Esaki, K. Soda, M. Tokushige, N. Yumoto, Purification and characterization of thermostable aspartase from *Bacillus* sp. YM55-1, Arch. Biochem. Biophys. 366 (1999) 40–46.
[11] T. Fujii, H. Sakai, Y. Kawata, Y. Hata, Crystal structure of thermostable aspartase from *Bacillus* sp. YM55-1: structure-based exploration of functional sites in the aspartase family, J. Mol. Biol. 328 (2003) 635–654.
[12] B. Weiner, G.J. Poelarends, D.B. Janssen, B.L. Feringa, Biocatalytic enantioselective synthesis of N-substituted aspartic acids by aspartate ammonia lyase, Chem. Eur. J. 14 (2008) 10094–10100.
[13] M. Tsai, J. Koo, P. Yip, R.F. Colman, M.L. Segall, P.L. Howell, Substrate and product complexes of *Escherichia coli* adenylosuccinate lyase provide new insights into the enzymatic mechanism, J. Mol. Biol. 370 (2007) 541–554.
[14] L.M. Sampaleanu, B. Yu, P.L. Howell, Mutational analysis of duck δ2 crystallin and the structure of an inactive mutant with bound substrate provide insight into the enzymatic mechanism of argininosuccinate lyase, J. Biol. Chem. 277 (2002) 4166–4175.
[15] A.R. Chakraborty, A. Davidson, P.L. Howell, Mutational analysis of amino acid residues involved in argininosuccinate lyase activity in duck δII crystallin, Biochemistry 38 (1999) 2435–2443.
[16] T. Weaver, L. Banaszak, Crystallographic studies of the catalytic and a second site in fumarase C from *Escherichia coli*, Biochemistry 35 (1996) 13955–13965.
[17] C.Y. Wu, H.J. Lee, S.H. Wu, S.T. Chen, S.H. Chiou, G.G. Chang, Chemical mechanism of the endogenous argininosuccinate lyase activity of duck lens δ2-crystallin, Biochem. J. 333 (1998) 327–334.
[18] I.I. Nuiry, J.D. Hermes, P.M. Weiss, C.Y. Chen, P.F. Cook, Kinetic mechanism and location of rate-determining steps for aspartase from *Hafnia alvei*, Biochemistry 23 (1984) 5168–5175.
[19] M.Y. Yoon, K.A. Thayer-Cook, A.J. Berdis, W.E. Karsten, K.D. Schnackerz, P.F. Cook, Acid-base chemical mechanism of aspartase from *Hafnia alvei*, Arch. Biochem. Biophys. 320 (1995) 115–122.
[20] A. Warshel, M. Levitt, Theoretical studies of enzymic reactions: dielectric, electrostatic and steric stabilization of the carbonium ion in the reaction of lysozyme, J. Mol. Biol. 103 (1976) 227–249.
[21] M.J. Field, P.A. Bash, M. Karplus, A combined quantum mechanical and molecular mechanical potential for molecular dynamics simulations, J. Comput. Chem. 11 (1990) 700–733.
[22] H.M. Senn, W. Thiel, QM/MM methods for biomolecular systems, Angew. Chem. Int. Ed. 48 (2009) 1198–1229.
[23] J.L. Gao, S.H. Ma, D.T. Major, K. Nam, J.Z. Pu, D.G. Truhlar, Mechanisms and free energies of enzymatic reactions, Chem. Rev. 106 (2006) 3188–3209.
[24] R.B. Wu, S.L. Wang, N.J. Zhou, Z.X. Cao, Y.K. Zhang, A proton-shuttle reaction mechanism for histone deacetylase 8 and the catalytic role of metal ions, J. Am. Chem. Soc. 132 (2010) 9471–9479.
[25] G.S. Sirin, Y.Z. Zhou, L. Lior-Hoffmann, S.L. Wang, Y.K. Zhang, Aging mechanism of soman inhibited acetylcholinesterase, J. Phys. Chem. B 116 (2012) 12199–12207.
[26] K. Doitomi, T. Kamachi, T. Toraya, K. Yoshizawa, Inactivation mechanism of glycerol dehydration by diol dehydratase from combined quantum mechanical/molecular mechanical calculations, Biochemistry 51 (2012) 9202–9210.
[27] Y.W. Li, L. Ding, Q.Z. Zhang, W.X. Wang, MD and QM/MM study on catalytic mechanism of a FAD-dependent enzyme ORF36: for nitro sugar biosynthesis, J. Mol. Graph. Model. 44 (2013) 9–16.
[28] A. Barman, R. Prabhakar, Elucidating the catalytic mechanism of β-secretase (BACE1): a quantum mechanics/molecular mechanics (QM/MM) approach, J. Mol. Graph. Model. 40 (2013) 1–9.
[29] M.H.M. Olsson, C.R. Søndergard, M. Rostkowski, J.H. Jensen, PROPKA3: consistent treatment of internal and surface residues in empirical p*K*a predictions, J. Chem. Theory Comput. 7 (2011) 525–537.
[30] W.A. Humphrey, K. Dalke, V.M.D. Schulten, Visual molecular dynamics, J. Mol. Graph. 14 (1996) 33–38.
[31] B.R. Brooks, R.E. Bruccoleri, B.D. Olafson, D.J. States, S. Swaminathan, M. Karplus, CHARMM: a program for macromolecular energy, minimization, and dynamics calculations, J. Comput. Chem. 4 (1983) 187–217.
[32] W.L. Jorgensen, J. Chandrasekhar, J.D. Madura, R.W. Impey, M.L. Klein, Comparison of simple potential functions for simulating liquid water, J. Chem. Phys. 79 (1983) 926–935.
[33] A.D. MacKerell Jr., D. Bashford, M. Bellott, R.L. Dunbrack Jr., J.D. Evanseck, M.J. Field, S. Fischer, J. Gao, H. Guo, S. Ha, D. Joseph-McCarthy, L. Kuchnir, K. Kuczera, F.T.K. Lau, C. Mattos, S. Michnick, T. Ngo, D.T. Nguyen, B. Prodhom, W.E. Reiher, B. Roux, M. Schlenkrich, J.C. Smith, R. Stote, J. Straub, M. Watanabe, J. Wiorkiewicz-Kuczera, D. Yin, M. Karplus, All-atom empirical potential for molecular modeling and dynamics studies of proteins, J. Phys. Chem. B 102 (1998) 3586–3616.
[34] P. Sherwood, A.H. de Vries, M.F. Guest, G. Schreckenbach, C.R.A. Catlow, S.A. French, A.A. Sokol, S.T. Bromley, W. Thiel, A.J. Turner, S. Billeter, F. Terstegen, S. Thiel, J. Kendrick, S.C. Rogers, J. Casci, M. Watson, F. King, E. Karlsen, M. Sjøvoll, A. Fahmi, A. Schäfer, C. Lennartz, QUASI: a general purpose implementation of the QM/MM approach and its application to problems in catalysis, J. Mol. Struct. Theochem. 632 (2003) 1–28.
[35] M. Berkowitz, J.A. McCammon, Molecular dynamics with stochastic boundary conditions, Chem. Phys. Lett. 90 (1982) 215–217.
[36] R. Ahlrichs, M. Bär, M. Häser, H. Horn, C. Kölmel, Electronic structure calculations on workstation computers: the program system turbomole, Chem. Phys. Lett. 162 (1989) 165–169.
[37] X.L. Pan, F.C. Cui, W. Liu, J.Y. Liu, QM/MM study on the catalytic mechanism of heme-containing aliphatic aldoxime dehydratase, J. Phys. Chem. B 116 (2012) 5689–5693.
[38] Z. Wang, S. Ferrer, V. Moliner, A. Kohen, QM/MM calculations suggest a novel intermediate following the proton abstraction catalyzed by thymidylate synthase, Biochemistry 52 (2013) 2348–2358.
[39] W. Smith, T.R. Forester, DL_POLY_2.0: a general-purpose parallel molecular dynamics simulation package, J. Mol. Graph. 14 (1996) 136–141.
[40] D. Bakowies, W. Thiel, Hybrid models for combined quantum mechanical and molecular mechanical approaches, J. Phys. Chem. 100 (1996) 10580–10594.
[41] S.R. Billeter, A.J. Turner, W. Thiel, Linear scaling geometry optimisation and transition state search in hybrid delocalised internal coordinates, Phys. Chem. Chem. Phys. 2 (2000) 2177–2186.